Non-isothermal Studies of Adduct Molecules of Metallic Halides with Oxo-Compounds in Solid State. I.

N. Ray CHAUDHURI, S. MITRA, and G. K. PATHAK

Inorganic Chemistry Laboratory, Indian Association for the Cultivation of Science, Calcutta 700032, India

(Received August 23, 1974)

Non-isothermal studies of some adduct molecules of metallic halides with dioxane as the type $MX_2 \cdot y$(dioxane) in solid state, where M=Mn(II), Co(II), Ni(II), Cu(II), Zn(II) or Cd(II), X=Cl^- or Br^- and y=0.5—2, were carried out with a Derivatograph. These inorganic adduct molecules lose dioxane molecule in single or multiple steps on heating. Thermally stable intermediate products were isolated and characterised by elemental analysis and IR spectra. The activation energy for each step of decomposition of the adduct was evaluated from the analysis of TG, DTG and DTA curves. Enthalpy change was evaluated from the DTA peak area and the order of reaction was found to be unity for each step of decomposition. Thermal stability of the adducts was discussed.

The preparation and characterisation of inorganic adduct molecule with dioxane have been done by several groups of workers.[1-17] Recently, Barnes and Duncan[18,19] carried out thermal decomposition of dioxane adducts of some metal halides. They investigated the thermal properties of the adducts by thermogravimetry, differential enthalpic analyses *etc.*, but not by the simultaneous measurements of TG, DTG and DTA, and they did not evaluate activation energy and order of reaction for each step of decomposition of the dioxane adducts. The present work deals with thermal decomposition of several known and unknown dioxane adducts of some metal halides. The evaluation of activation energy for the decomposition of adducts was worked out simultaneously from TG, DTG and DTA curves. In addition to the evaluation of activation energy of decomposition, the present paper deals with the evaluation of order of reaction (n) and ΔH from DTA peak area. It also shows the effect on the change of cation and anion on the thermal properties of dioxane adducts.

Experimental

For the preparation of dioxane adducts of metal halides anhydrous dioxane in excess was added to the finely powdered anhydrous metal halides and the mixture was stirred for 24—48 hr under dry conditions. The mixture was kept in desiccator for slow evaporation of the excess dioxane. All the adducts were characterized by elemental analysis. The dioxane used was sufficiently purified and dried according to the standard procedure.[20]

The following adducts of metal halides were prepared:
1. $MnCl_2 \cdot 1D$ 2. $MnBr_2 \cdot 2D$ 3. $CoCl_2 \cdot 0.5D$ 4. $CoBr_2 \cdot 2D$
5. $NiCl_2 \cdot 1.5D$ 6. $NiBr_2 \cdot 2D$ 7. $NiBr_2 \cdot 1D$ 8. $CuCl_2 \cdot 0.75D$
9. $CuBr_2 \cdot 2D$ 10. $ZnBr_2 \cdot 1D$ 11. $CdCl_2 \cdot 0.5D$ 12. $CdBr_2 \cdot 1D$
where D denotes dioxane molecule.

A Paulik-Paulik-Erdey type MOM Derivatograph was used for thermal analysis. The particle size of the sample was within 150—200 mesh. Heating rate was about 1.5 °C/min. The volume of the sample in each case was same. Platinum crucible was used for thermal analysis. All these experiments were conducted in static air.

Results

The dioxane adducts of $MnCl_2$, $CoCl_2$, $NiCl_2$, $NiBr_2$, $CuCl_2$, $ZnBr_2$, $CdCl_2$, and $CdBr_2$ lose all dioxane molecules in a single step which is evident from their respective TG, DTG and DTA curves (Figs. 1—4). The adduct $MnBr_2 \cdot 2D$ loses dioxane molecule in two distinct steps forming stable $MnBr_2 \cdot 1D$ as an intermediate. $CoBr_2 \cdot 2D$ loses dioxane molecules in three steps, *i.e.*,

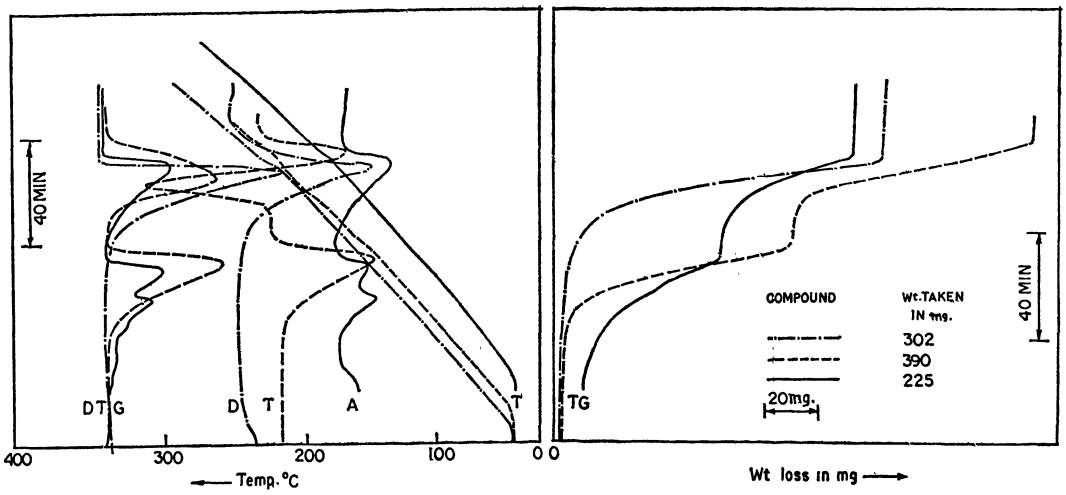

Fig. 1. The derivatograms for $MnCl_2 \cdot 1D$ (—·—·—), $MnBr_2 \cdot 2D$ (————) and $CoBr_2 \cdot 2D$ (————).

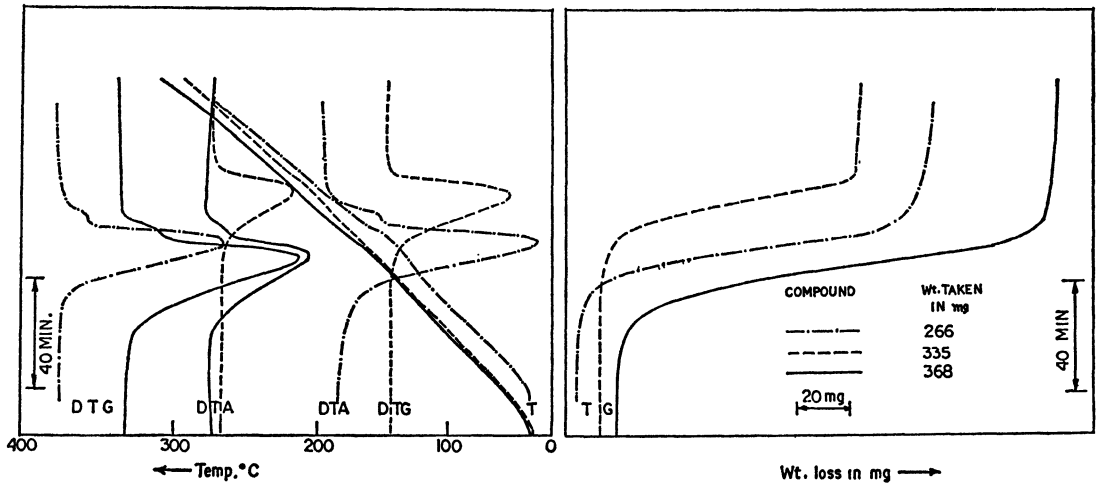

Fig. 2. The derivatograms for $NiCl_2 \cdot 1.5D$ (—·—·—), $NiBr_2 \cdot 1D$ (———) and $NiBr_2 \cdot 2D$ (———).

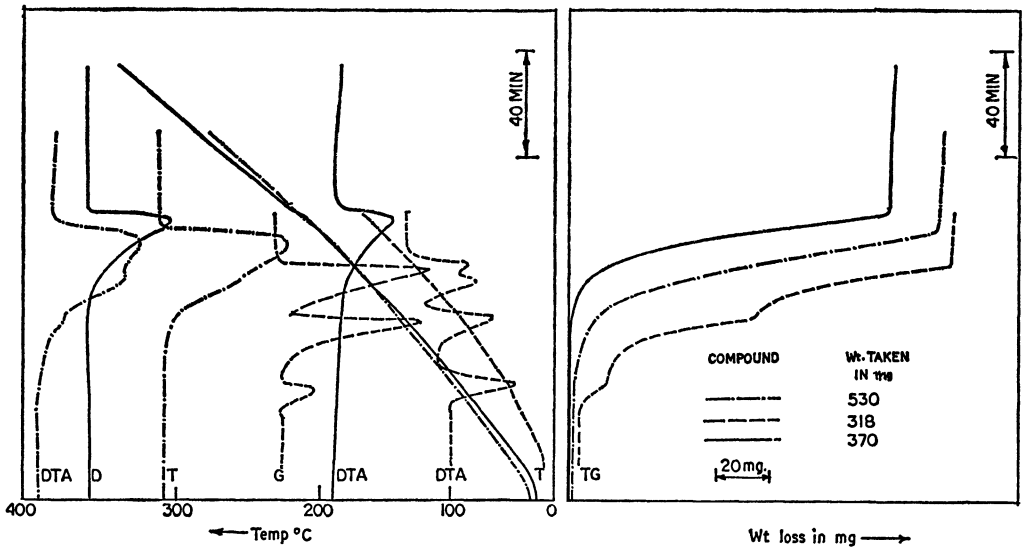

Fig. 3. The derivatograms for $CoCl_2 \cdot 0.5D$ (—·—·—), $CuBr_2 \cdot 2D$ (———) and $CuCl_2 \cdot 0.75D$ (———).

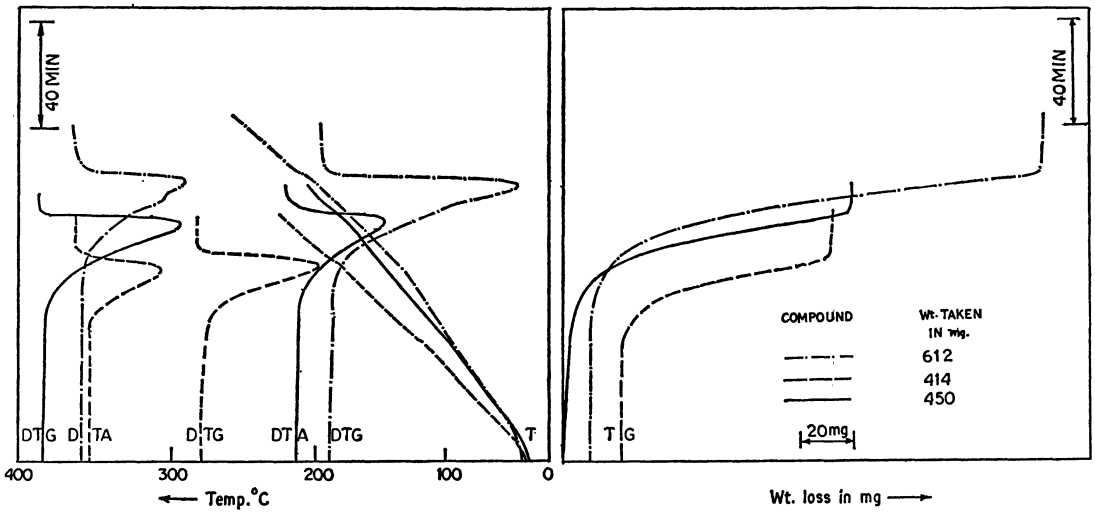

Fig. 4. The derivatograms for $ZnBr_2 \cdot 1D$ (—·—·—), $CdCl_2 \cdot 0.5D$ (———) and $CdBr_2 \cdot 1D$ (———).

$$CoBr_2\cdot 2D \xrightarrow{-0.5D} CoBr_2\cdot 1.5D \xrightarrow{-0.5D}$$
$$CoBr_2\cdot 1D \xrightarrow{-1D} CoBr_2$$

The first decomposition product $CoBr_2\cdot 1.5D$ is very unstable and second one is stable which is evident from its derivatogram (Fig. 1). Whereas, $CuBr_2\cdot 2D$ loses dioxane molecules in three steps, *i.e.*,

$$CuBr_2\cdot 2D \xrightarrow{-0.2D} CuBr_2\cdot 1.8D \xrightarrow{-0.8D}$$
$$CuBr_2\cdot 1D \xrightarrow{-1D} CuBr_2$$

All the intermediate products are unstable. DTA curve for the decomposition process of $CuBr_2\cdot 1D \rightarrow CuBr_2$ (Fig. 3) shows two overlapped endotherms. Whereas, its DTG curve indicates a single step of decomposition.

The decomposition of the adducts shows endotherm, except for tha of $MnBr_2\cdot 1D$ which shows an exotherm just followed by an endotherm in DTA curve. Temperature ranges of decomposition and the DTG peak temperatures for the adducts are listed in the second and third columns in Table 1, respectively.

Enthalpy change for each step of decomposition of the adducts was evaluated by the method of Sano[21,22] using copper sulfate pentahydrate as the standard and the values are tabulated in the last column in Table 1. When the two DTA peaks were too much overlapped with each other, the ΔH values were evaluated from the overall area of the DTA peaks concerned.

The activation energy for each step of decomposition of the adduct molecules was evaluated from the analysis of TG curves using Freeman and Carroll's[23] equation:

$$\frac{E_a}{2.3R}\Delta T^{-1}\Big/\Delta \log W_r = -n + \Delta \log \frac{dw}{dt}\Big/\Delta \log W_r,$$

where E_a is activation energy, n is order of reaction, T is absolute temperature, t is time, dw/dt is rate of weight loss with time, R is gas constant and W_r is weight loss at completion of reaction minus weight loss upto time t. The values are given in Table 1 and the corresponding curves are shown in Figs. 5 and 6. The order of reaction for each step of decomposition is unity.

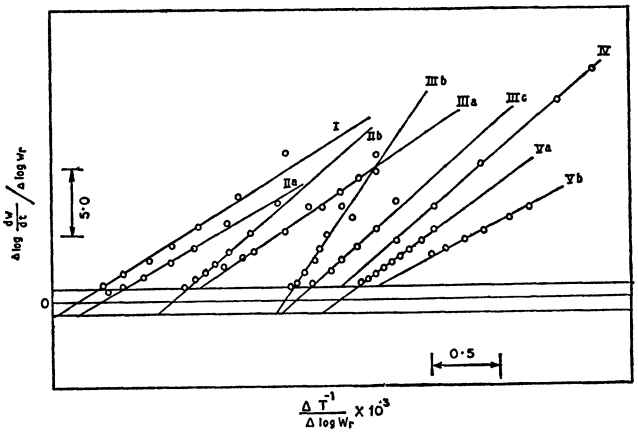

Fig. 5. Plots of $\Delta\log(dw/dt)/\Delta\log W_r$ *vs.* $\Delta T^{-1}/\Delta\log W_r \times 10^3$ from TG for the decomposition of $MnCl_2\cdot 1D \rightarrow MnCl_2$(I), $MnBr_2\cdot 2D \rightarrow MnBr_2\cdot 1D$(IIa), $MnBr_2\cdot 1D \rightarrow MnBr_2$(IIb), $CoBr_2\cdot 2D \rightarrow CoBr_2\cdot 1.5D$(IIIa), $CoBr_2\cdot 1.5D \rightarrow CoBr_2\cdot 1D$(IIIb), $CoBr_2\cdot 1D \rightarrow CoBr_2$(IIIc), $NiCl_2\cdot 1.5D \rightarrow NiCl_2$(IV), $NiBr_2\cdot 1D \rightarrow NiBr_2$(Va) and $NiBr_2\cdot 2D \rightarrow NiBr_2$(Vb).

Table 1. Thermal parameters for the decomposition of adduct molecules of some metallic halides with dioxane

	Decomposition reaction	Temp. range °C	DTG peak temp. °C	Activation energy E_a kcal/mol			Enthalpy change ΔH kcal/mol
				TG	DTG	DTA	
1.	$MnCl_2\cdot 1D \longrightarrow MnCl_2$	147.5—226	216	28.75	33.73	32.85	24.03
2a.	$MnBr_2\cdot 2D \longrightarrow MnBr_2\cdot 1D$	90 —155	142.5	26.83	28.75	28.75	12.51
b.	$MnBr_2\cdot 1D \longrightarrow MnBr_2$	170 —235	212	38.33	38.33	b)	b)
3.	$CoCl_2\cdot 0.5D \longrightarrow CoCl_2$	124.5—200	192	28.75	28.75	c)	20.59
4a.	$CoBr_2\cdot 2D \longrightarrow CoBr_2\cdot 1.5D$	30 — 80	83	30.60	c)	c)	20.74[a]
b.	$CoBr_2\cdot 1.5D \longrightarrow CoBr_2\cdot 1D$	84 —110	105	69.00	c)	c)	
c.	$CoBr_2\cdot 1D \longrightarrow CoBr_2$	128 —185	178	39.42	39.42	39.42	18.15
5.	$NiCl_2\cdot 1.5D \longrightarrow NiCl_2$	89 —205	144.5	34.50	34.50	34.50	32.86
6.	$NiBr_2\cdot 2D \longrightarrow NiBr_2$	84 —195	157.5	23.00	25.10	25.10	12.61
7.	$NiBr_2\cdot 1D \longrightarrow NiBr_2$	147.5—220	204	32.85	39.40	38.90	12.36
8.	$CuCl_2\cdot 0.75D \longrightarrow CuCl_2$	132 —217	209	31.50	31.50	31.50	7.76
9a.	$CuBr_2\cdot 2D \longrightarrow CuBr_2\cdot 1.8D$	36 — 50	50	c)	c)	c)	47.57
b.	$CuBr_2\cdot 1.8D \longrightarrow CuBr_2\cdot 1D$	55 — 93	89	34.50	38.30	38.30	14.16
c.	$CuBr_2\cdot 1D \longrightarrow CuBr_2$	93 —130	126	38.14	38.14	III	11.33
10.	$ZnBr_2\cdot 1D \longrightarrow ZnBr_2$	112 —224	200	26.20	26.20	26.20	11.73
11.	$CdCl_2\cdot 0.5D \longrightarrow CdCl_2$	120 —190	177	57.50	57.50	57.50	13.54
12.	$CdBr_2\cdot 1D \longrightarrow CdBr_2$	120 —185	177	30.66	30.66	30.66	16.24

a) Indicates overall enthalpy change. b) Activation energy and enthalpy change from DTA curve could not be evaluated due to irregular nature of the DTA peaks. c) Evaluation of activation energy was not possible due to much overlapping of the curves with each other.

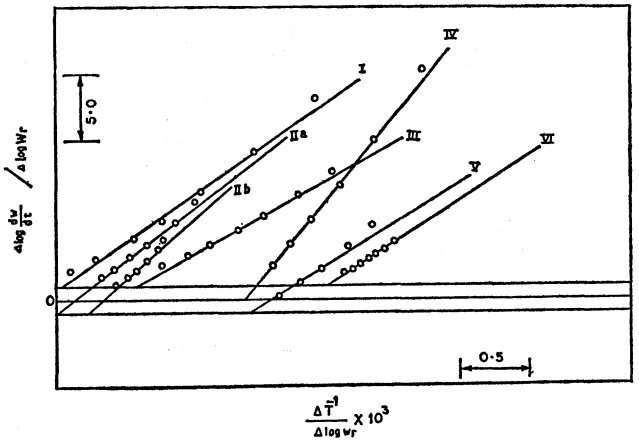

Fig. 6. Plots of $\Delta\log(dw/dt)/\Delta\log W_r$ *vs.* $\Delta T^{-1}/\Delta\log W_r \times 10^3$ from TG for the decomposition of $CuCl_2\cdot 0.75D \rightarrow CuCl_2$(I), $CuBr_2\cdot 1.8D \rightarrow CuBr_2\cdot 1D$(IIa), $CuBr_2\cdot 1D \rightarrow CuBr_2$(IIb), $ZnBr_2\cdot 1D \rightarrow ZnBr_2$(III), $CdCl_2\cdot 0.5D \rightarrow CdCl_2$(IV), $CdBr_2\cdot 1D \rightarrow CdBr_2$(V) and $CoCl_2\cdot 0.5D \rightarrow CoCl_2$(VI).

Activation energy for each step of decomposition was determined from the analysis of DTG curve using the method of Dave and Chopra.[24]

$$k = \frac{\left(\frac{A}{N_0}\right)^{n-1}\left(-\frac{dx}{dt}\right)}{(A-a)^n}$$

where N_0 is number of mol of sample at time t at which the DTG peak begins to appear, A and a are the total peak area and the area swept out till the time t, respectively, dx/dt is the displacement of the DTG curve from the base line and n is the order of reaction. The determination of order of reaction by this method is a trial and error process which amounts to calculating the rate constants corresponding to different values of n and finding out the best fitting curve for the Arrhenius plot which gives the value of n. In our work we found that by putting the value of the order of reaction $n=1$ (calculated from TG curve), we got the best fitting Arrhenius plot in all the cases. As a result

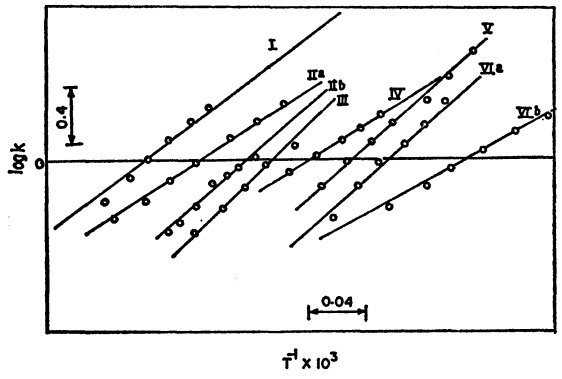

Fig. 7. Arrhenius plots, $\log k$ *vs.* $T^{-1}\times 10^3$, from DTG for the decomposition of $MnCl_2\cdot 1D \rightarrow MnCl_2$(I), $MnBr_2\cdot 2D \rightarrow MnBr_2\cdot 1D$(IIa), $MnBr_2\cdot 1D \rightarrow MnBr_2$(IIb), $CoBr_2\cdot 1D \rightarrow CoBr_2$(III), $CoCl_2\cdot 0.5D \rightarrow CoCl_2$(IV), $NiCl_2\cdot 1.5D \rightarrow NiCl_2$(V), $NiBr_2\cdot 1D \rightarrow NiBr_2$(VIa) and $NiBr_2\cdot 2D \rightarrow NiBr_2$(VIb).

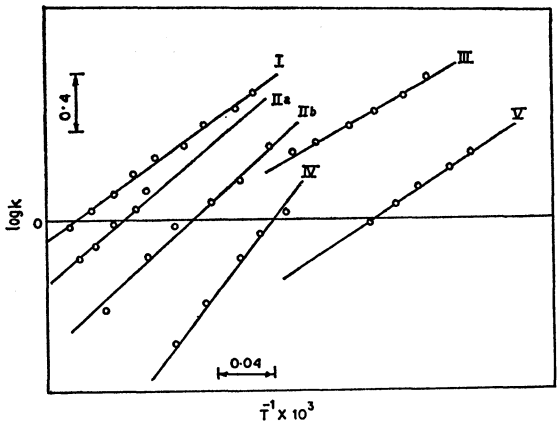

Fig. 8. Arrhenius plots, $\log k$ *vs.* $T^{-1}\times 10^3$, from DTG for the decomposition of $CuCl_2\cdot 0.75D \rightarrow CuCl_2$(I), $CuBr_2\cdot 1.8D \rightarrow CuBr_2\cdot 1D$(IIa), $CuBr_2\cdot 1D \rightarrow CuBr_2$(IIb), $ZnBr_2\cdot 1D \rightarrow ZnBr_2$(III), $CdCl_2\cdot 0.5D \rightarrow CdCl_2$(IV) and $CdBr_2\cdot 1D \rightarrow CdBr_2$(V).

we did not have to use the laborious trial and error method of Dave and Chopra. The values of the activation energies are given in Table 1 and the curves are shown in Figs. 7 and 8. We could not determine the activation energy by this method in some cases where the curves are too much overlapped.

Activation energy for each step of decomposition was also determined from the analysis of DTA curves using Brochardt equation[25] for first order reaction

$$k = \frac{C_p\frac{d\Delta T}{dt} + K\Delta T}{K(A-a) - C_p\Delta T}$$

where k is rate constant for the reaction, A is total DTA area, C_p is total heat capacity, K is cell constant, a is area at time t, $d\Delta T/dt$ expresses slope of the DTA curve at time t, ΔT is the displacement of the DTA curve from the base line at time t. As quantities $C_p\, d\Delta T/dt$ and $C_p\Delta T$ are, in general, small, the equa-

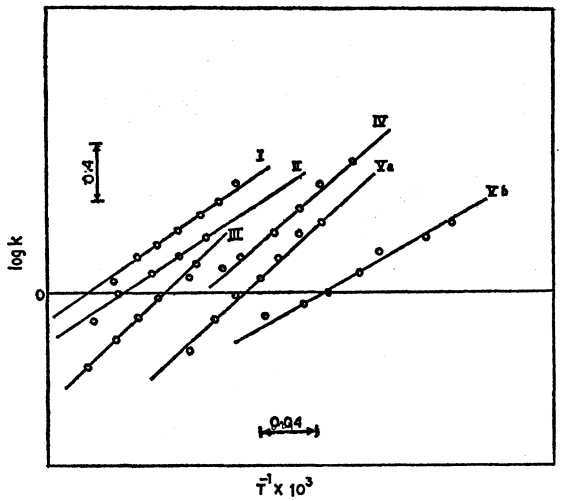

Fig. 9. Arrhenius plots, $\log k$ *vs.* $T^{-1}\times 10^3$, from DTA for the decomposition of $MnCl_2\cdot 1D \rightarrow MnCl_2$(I), $MnBr_2\cdot 2D \rightarrow MnBr_2\cdot 1D$(II), $CoBr_2\cdot 1D \rightarrow CoBr_2$(III), $NiCl_2\cdot 1.5D \rightarrow NiCl_2$(IV), $NiBr_2\cdot 1D \rightarrow NiBr_2$(Va) and $NiBr_2\cdot 2D \rightarrow NiBr_2$(Vb).

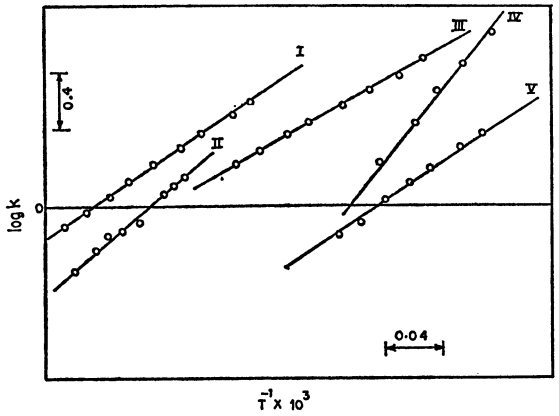

Fig. 10. Arrhenius plots, $\log k$ *vs.* $T^{-1}\times 10^3$, from DTA for the decomposition of $CuCl_2\cdot 0.75D \rightarrow CuCl_2$(I), $CuBr_2\cdot 1.8D \rightarrow CuBr_2\cdot 1D$(II), $ZnBr_2\cdot 1D \rightarrow ZnBr_2$-(III), $CdCl_2\cdot 0.5D \rightarrow CdCl_2$(IV) and $CdBr_2\cdot 1D \rightarrow CdBr_2$(V).

tion reduces to $k=\Delta T/(A-a)$. From the plot of $\log k$ *vs.* T^{-1} activation energy can easily be evaluated. The values are tabulated in Table 1 and the curves are shown in Figs. 9 and 10. Here also we could not determine the activation energy in some cases for too much overlapping of the DTA curves.

IR spectra of the adducts were taken to ensure the presence of dioxane molecule in the adducts.

Discussion

According to the observations by Barnes and Duncan[19] the adduct $MnBr_2\cdot 2D$ loses all dioxane molecules in single step showing two overlapped endotherm. They could not isolate the intermediate product of composition $MnBr_2\cdot 1D$. Whereas, we observed well-resolved DTA peaks for the two decomposition steps of $MnBr_2\cdot 2D$ to $MnBr_2\cdot 1D$ and of $MnBr_2\cdot 1D$ to $MnBr_2$, the former showing an endotherm and the latter showing an exotherm followed by an endotherm in the DTA curve (Fig. 1). But the corresponding TG and DTG curves for the decomposition of $MnBr_2\cdot 1D$ to $MnBr_2$ do not show any intermediate step. Earlier, dioxane adduct of $CoCl_2$ was known as $CoCl_2\cdot 1D$. On the contrary, we isolated the adduct as $CoCl_2\cdot 0.5D$ alone. The existence of $CoBr_2\cdot 1.5D$, though not stable, was not pointed out earlier.[19] We isolated the adduct of $NiCl_2$ as $NiCl_2\cdot 1.5D$, whereas, the composition of the adduct of the same salt was reported earlier[19] as $NiCl_2\cdot 1D$. We could not isolate $NiBr_2\cdot 1D$ from the thermal decomposition of $NiBr_2\cdot 2D$ but isolated the same by keeping $NiBr_2\cdot 2D$ in a vacuum desiccator for a long time. In case of $CuCl_2$ we repeatedly isolated the adduct $CuCl_2\cdot 0.75D$ alone and never obtained 3 $CuCl_2\cdot 2D$ and $CuCl_2\cdot 2D$ reported earlier.[18] Whereas, dioxane adduct of $CuBr_2$ was reported by the same workers[19] as 3 $CuBr_2\cdot 2D$ which showed single step of thermal decomposition. But we isolated the adduct as $CuBr_2\cdot 2D$. In literature[1,19] two dioxane adducts such as $CdCl_2\cdot 0.5D$ and $CdCl_2\cdot 1D$ were reported. We could not isolate $CdCl_2\cdot 1D$. The thermal decomposition of $CdCl_2\cdot 1D$ reported earlier[19] did not show the existence of $CdCl_2\cdot 0.5D$ from TG at any temperature.

The partial disagreement in our observations with those of the aforementioned works is possibly due to the difference in experimental conditions employed. Particular mention may be made of the wide difference of heating rate, *i.e.*, 8—10 °C/min used in the earlier works[19] compared to that of 1.5 °C/min used in our experiments.

DTG peak temperature for a series of adducts of the type $MBr_2(dioxane)_2$, where M is Mn(II), Co(II), Ni(II) or Cu(II), increases in the order: Cu(II) <Co(II) <Mn(II) <Ni(II) and for a series of adducts of the type MX_2dioxane, where M is Mn(II), Co(II), Ni(II), Cu(II), Zn(II) or Cd(II) and X is Cl^- or Br^-, increases in the order Cu(II) <Cd(II) <Co(II) <Zn(II) <Ni(II) <Mn(II). A similar order was found in the case of the decomposition of some pyridine 1-oxide coordination compounds.[26] Of the dioxane adducts of the halides of bivalent transition metal ion like Mn(II), Co(II), Ni(II) or Cu(II), the Mn(II) compound is thermally most stable. Among these metal ions Mn(II) is the hardest acceptor and oxygen donors like dioxane are hard donors. Naturally, dioxane will form the strongest donor acceptor bond with Mn(II) which is the hardest acceptor of the above series and the highest energy will be required to rupture the Mn(II)–dioxane bond.

It was observed that dioxane adduct of metal bromide is thermally less stable than the corresponding adduct of metal chloride. The value of enthalpy change for the decomposition of $CuBr_2\cdot 1.8D \rightarrow CuBr_2\cdot 1D$ is smaller than that for the first step of decomposition $CuBr_2\cdot 2D \rightarrow CuBr_2\cdot 1.8D$, though, in general, the latter step of decomposition gives larger ΔH value than the earlier step. It is noticed that the value of enthalpy change ranges from 7 to 47.5 kcal/mol.

Activation energies evaluated from TG, DTA and DTG do not differ much from each other, which shows that all the methods used for the evaluation of activation energies are standard. The differences in the activation energies of decomposition between the adducts do not show any systematic relationships with the kind or the nature of either cation (*i.e.*, the electronic configuration of the metal ion) or the anion.

In general, DTA curve shows endotherm for the decomposition of the similar type of adducts. This is seen in the decomposition of all the adducts except the decomposition of $MnBr_2\cdot 1D \rightarrow MnBr_2$. Its nature of DTA and the corresponding TG and DTG curves possibly indicates some kinds of structural rearrangement at the beginning of the decomposition. The evolution of heat due to this rearrangement probably overcomes the endothermic effect due to decomposition at the beginning. This may explain the exotherm observed in the DTA curve.

The authors wish to express their hearty thanks to Dr. S.P. Ghosh, Research Officer of this laboratory for his kind discussion.

References

1) Sr. R. Juhasz and L. F. Yntema, *J. Amer. Chem. Soc.*, **62**, 3522 (1940).

2) P. M. Hamilton, R. Mcbeth, W. Bekebrede, and H. H. Sisler, *ibid.*, **75**, 2881 (1953).
3) A. E. Comyns and H. J. Lucas, *ibid.*, **76**, 1019 (1954).
4) R. F. Rolsten and H. H. Sisler, *ibid.*, **79**, 1068 (1957).
5) P. A. Mccusker, T. J. Lane, and S. M. S. Kennard, *ibid.*, **81**, 2974 (1959).
6) P. J. Kendra and D. B. Powell, *J. Chem. Soc.*, **1960**, 5105.
7) G. Vicentini, M. Perrier, and E. Giesbrecht, *Chem. Ber.*, **94**, 1153 (1961).
8) G. Vicentini, M. Perrier, W. G. R. DeCamargo, and J. M. V. Coutinho, *ibid.*, **94**, 1063 (1961).
9) M. Perrier, E. Giesbrecht, W. G. R. DeCamargo, and G. Vicentini, *ibid.*, **95**, 257 (1962).
10) A. M. Golub, O. O. Pisakaro'va, and L. D. Bogats'ka, *Fiz. ta Khim.*, **1**, 78 (1961).
11) G. Vicentini, J. V. Valarelli, M. Perrier, and E. Giesbrecht, *J. Inorg. Nucl. Chem.*, **24**, 1351 (1962).
12) E. Giesbrecht, W. G. R. DeCamargo, G. Vicentini, and M. Perrier, *ibid.*, **24**, 381 (1962).
13) G. Vicentini, M. Perrier, and E. Giesbrecht, *ibid.*, **26**, 2207 (1964).
14) B. E. Bridgland, G. W. A. Fowles, and R. A. Walton, *ibid.*, **27**, 383 (1965).
15) T. Gruhn and M. Gorman, *ibid.*, **27**, 482 (1965).
16) G. W. A. Fowles, D. A. Rice, and R. A. Walton, *J. Chem. Soc., A*, **1968**, 1842.
17) R. C. Maheshwari, S. K. Suri, and V. Ramakrishna, *Ind. J. Chem.*, **11**, 1196 (1973).
18) J. C. Barnes, *J. Inorg. Nucl. Chem.*, **31**, 95 (1969).
19) J. C. Barnes and C. S. Duncan, *J. Chem. Soc., A*, **1970**, 1442; **1972**, 923.
20) L. F. Fieser, "Experiments in Organic Chemistry," Second Ed., D. C. Heath and Co., Boston (1969), p. 368.
21) K. Sano, *Sci. Rep. Tohoku. Imp. Univ. 1st Ser.*, **24**, 719 (1936).
22) R. Tsuchiya, Y. Kaji, A. Uehara, and E. Kyuno, This Bulletin, **42**, 1881 (1969).
23) E. S. Freeman and B. Carroll, *J. Phys. Chem.*, **62**, 394 (1958).
24) N. G. Dave and S. K. Chopra, *Z. Phys. Chem.*, **48**, 257 (1966).
25) H. J. Brochardt and F. Daniels, *J. Amer. Chem. Soc.*, **79**, 41 (1957).
26) A. J. Pappas, F. A. Osterman, Jr., and H. B. Powell, *Inorg. Chem.*, **9**, 2695 (1970).